

# Raman Investigation of Surface OH-Species in Porous Silica

Alberto Anedda, Carlo M. Carbonaro,\* Francesca Clemente, Riccardo Corpino, and P. Carlo Ricci

Dipartimento di Fisica, Università di Cagliari, and INFM, UdR Cagliari, sp n° 8, Km 0,700, I-09042 Monserrato (CA), Italy

Received: September 9, 2003

Surface in porous media has a key role for both theoretical and technological aspects. A comparative analysis of the surface vibrational properties of sol–gel synthesized porous silica monoliths with different porosity is presented. Raman spectroscopy investigation of the fundamental O–H stretching range (3000–3800  $\text{cm}^{-1}$ ) reveals a dependence of the surface reactivity on pore dimensions. The pore surface curvature plays an important role affecting the hydrogen-bonding interaction between surface hydroxyls and modifying the distribution of the OH species at the surface; the relative contribution of interacting hydroxyls and adsorbed water with respect to isolated species is larger in smaller pores. Water and silanol vibrations were singled out as a function of porosity.

## 1. Introduction

Sol–gel synthesized porous silica surface is naturally terminated with a variety of surface silanols (isolated, geminal, and vicinal) which are preferential adsorption sites for water molecules. Surface hydroxyls are, indeed, particularly reactive species where  $\text{H}_2\text{O}$  and other polar molecules are likely to be physically adsorbed to form a multiply hydrogen-bonded layer.<sup>1–3</sup>

Aiming to obtain high-performing porous  $\text{SiO}_2$  devices (e.g., luminescent devices, gas sensors, solid dyes), the knowledge of the surface structure, morphology, and chemistry is a key aspect to control physical and chemical adsorption of guest molecules within porous silica.<sup>4–7</sup>

Porous silica properties are related to the concentration and distribution of hydroxyls at the surface. The chemistry of the porous silica surface and its chemical and physical interactions with the environment have been investigated through vibrational spectroscopies, thermogravimetric methods, and nuclear magnetic resonance (NMR) at different stages of the sol–gel synthesis.<sup>1,6–11</sup> The silica surface can be visualized as the truncation of a random network composed of siloxane (Si–O–Si) rings containing, on average, six atoms per ring. Open rings at the surface are generally terminated with OH groups bonded with a silicon atom, SiOH units (silanol) in the form of isolated, geminal, and vicinal structures.<sup>1,2</sup> The concentration of OH groups at the surface is about 4–5 OH/ $\text{nm}^2$  and it is found to be almost independent of the synthesis conditions of porous silica.<sup>1</sup> However, the hydrogen-bond interaction of OH groups at the surface is determined by the Si–O–Si ring size and its opening degree, the number of hydroxyls per silicon site, and the surface curvature.<sup>1</sup> In particular, a small negative curvature radius reduces the distance between neighbor hydroxyls and enhances the hydrogen-bond interaction with respect to a flat surface.<sup>1</sup> Thus, the smaller the pore diameter, the larger the expected interaction between silanols. Moreover, water should be preferentially adsorbed on complex interacting SiOH rather

than on isolated structures; a higher concentration of adsorbed water should be expected in smaller pore samples.<sup>1</sup>

Raman and infrared spectroscopies have been extensively used to investigate the vibrational properties of silica throughout the whole sol–gel synthesis. As regards the O–H fundamental stretching vibration, 3000–3800  $\text{cm}^{-1}$ , the broad vibrational band has been assigned to the superimposition of different bonded hydroxyl groups whereas the narrow feature peaked at 3750  $\text{cm}^{-1}$  has been identified as the fingerprint of the isolated silanol vibration.<sup>1,8–14</sup>

To determine the distribution of the hydroxyl groups at the porous silica surface and their possible correlation with the surface curvature of the pores, a comparative study on the vibrational properties of sol–gel synthesized porous silica is presented. Raman spectra (RS) of samples with different porosity are analyzed in the O–H stretching range; a dependence of the relative concentration of the different hydroxyl species on the mean pore diameter of the samples is observed. By taking into account the contribution of bulk water nested into the pores we singled out the effective role of surface SiOH groups.

## 2. Experimental Section

Raman Scattering measurements were performed with a Raman spectrometer (Dilor XY800). An argon ion laser operating at 514.5 nm (Coherent Innova 90C-4) supplied the excitation. The signal, dispersed with a 600 grooves/mm grating, was detected by a  $1024 \times 256$   $\text{LN}_2$  cooled charge coupled detector (CCD). All Raman scattering measurements were performed with a spectral resolution of  $\sim 2$   $\text{cm}^{-1}$ , at room temperature.

Measurements have been performed on sol–gel synthesized porous silica monoliths with different porosity produced by Geltech Inc. (US).

The first set of samples (hereafter A) has a pore diameter distribution sharply peaked at 3.2 nm (5% of standard deviation), a pore volume of 0.488  $\text{cm}^3 \text{g}^{-1}$  with a specific surface area of 594  $\text{m}^2 \text{g}^{-1}$ , and a density of about 1.2  $\text{g cm}^{-3}$ . The second set of samples (hereafter B) has a pore diameter distribution sharply peaked at 5.5 nm (5% of standard deviation), a pore volume of

\* Corresponding author. Phone: +390706754823. Fax: +39070510171. E-mail: cm.carbonaro@dsf.unica.it.

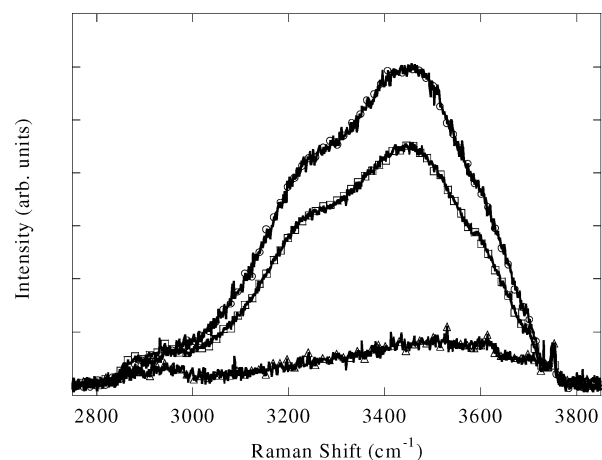


**Figure 1.** Raman Spectra in the fundamental O–H stretching range of samples A (circles), B (squares), and C (triangles).

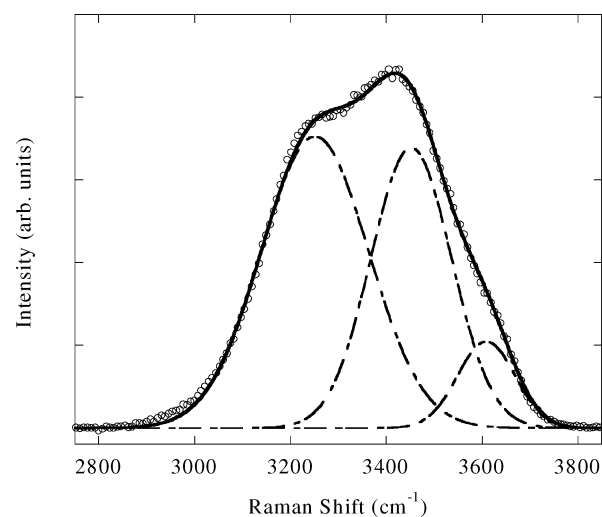


**Figure 2.** Best fit deconvolution ( $r^2 = 0.99$ ) of liquid water Raman spectrum in the O–H stretching range: markers are the experimental data, dashed lines are the Gaussian components according to the fitting analysis, and the solid line is the resulting fit.

$0.741 \text{ cm}^3 \text{ g}^{-1}$  with a specific surface area of  $540 \text{ m}^2 \text{ g}^{-1}$ , and a density of about  $0.9 \text{ g cm}^{-3}$ . The third set of samples (hereafter C) has a mean pore diameter of  $18.2 \text{ nm}$  (5% standard deviation), a pore volume of  $1.208 \text{ cm}^3 \text{ g}^{-1}$  with a specific surface area of  $264 \text{ m}^2 \text{ g}^{-1}$ , and a density of about  $0.6 \text{ g cm}^{-3}$ .<sup>15</sup>

### 3. Results

Raman spectra of the samples in the  $2750\text{--}3850 \text{ cm}^{-1}$  range are shown in Figure 1. The three sets of samples display a composite band in the  $2900\text{--}3800 \text{ cm}^{-1}$  range with a narrow feature at  $3750 \text{ cm}^{-1}$ . For a better comparison, spectra have been arbitrarily normalized to the  $3750 \text{ cm}^{-1}$  intensity peak. The contribution of the composite band in the  $2900\text{--}3800 \text{ cm}^{-1}$  range with respect to the  $3750 \text{ cm}^{-1}$  peak decreases as the pore diameter of the silica samples increases.

To take into account the contribution of liquid water nested into the pores, a Gaussian best-fit deconvolution<sup>16</sup> of the RS of distilled liquid water in the O–H stretching range is shown in Figure 2. Three Gaussian components peaked at  $3250$ ,  $3451$ , and  $3608 \text{ cm}^{-1}$  with  $264$ ,  $198$ , and  $141 \text{ cm}^{-1}$  as full width at half-maximum (fwhm), respectively, are found.

Porous silica Raman spectra have been tentatively resolved by using Gaussian bands and the reconstructed  $\text{H}_2\text{O}$  contribution. A variable concentration of “bulk” water within the pores has

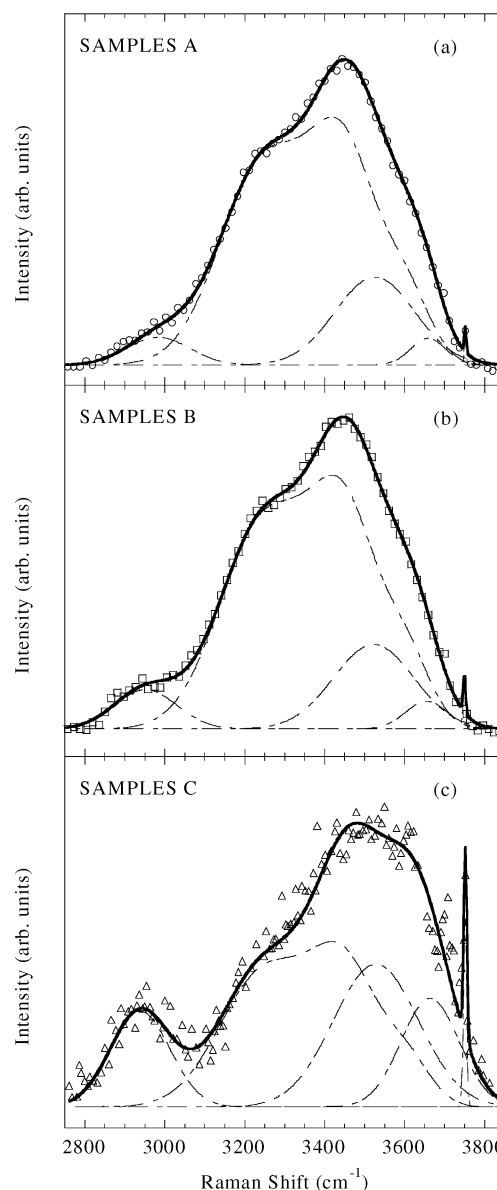


**Figure 3.** Best fit deconvolution of the Raman spectra in the O–H stretching range of (a) A samples; (b) B samples; (c) C samples. Markers are the experimental data, dashed lines are the Gaussian bands and the reconstructed water contribution according to the fitting analysis, and the solid line is the resulting fit.

been assumed; the liquid water best fit is constrained in position and shape and multiplied by a scaling factor parameter.

Figure 3 displays the deconvolution of the RS of the three sets of samples: upper (Figure 3a), central (Figure 3b), and lower (Figure 3c) panels report the deconvoluted RS of A, B, and C samples, respectively.

Besides the contribution of water, four Gaussian components are found and their peak positions and fwhm are reported in Table 1 with an estimated uncertainty of  $2 \text{ cm}^{-1}$ . The relative contribution of water and different Gaussian bands is estimated through the integrated area percentage reported in Table 2.

### 4. Discussion

The surface properties of silica are of great technological interest; adsorption occurring at the oxide surface influences the performance of silica-based devices. In porous silica—whose specific surface can be increased up to  $1000 \text{ m}^2 \text{ g}^{-1}$  in silica aerogels—the importance of surface phenomena is further

**TABLE 1: Spectral Properties of the Gaussian Bands of the Deconvoluted Spectra<sup>a</sup>**

sample	peak— fwhm (cm <sup>-1</sup> )	peak— fwhm (cm <sup>-1</sup> )	peak— fwhm (cm <sup>-1</sup> )	peak— fwhm (cm <sup>-1</sup> )	r <sup>2</sup>
A	2982–186	3525–235	3658–101	3751–7	0.99
B	2950–185	3522–237	3654–123	3749–8	0.99
C	2937–176	3527–251	3663–171	3751–10	0.92

<sup>a</sup> Spectral properties of the Gaussian bands and r<sup>2</sup> values for A, B and C samples.

**TABLE 2: Integrated Area Percentage of the Components of the Deconvoluted Spectra<sup>a</sup>**

sample	IA <sub>2960</sub> %	IA <sub>3525</sub> %	IA <sub>3658</sub> %	IA <sub>3750</sub> %	IA <sub>water</sub> %
A	4.0	15.9	2.1	0.1	77.9
B	5.4	14.8	2.5	0.2	77.0
C	11.7	25.0	13.0	1.3	49.0

<sup>a</sup> Integrated area percentage of the different components for the A, B, and C samples.

enhanced affecting the structural and optical properties of the material and the confinement of guest molecules in the silica matrix. The feasibility, stability, and performances of porous SiO<sub>2</sub> devices depend on surface activity and reactivity. A study of the distribution of the surface hydroxyl groups on the silica walls of samples having different mean pore diameters could give useful information, for example, in the choice of the suitable host for nonlinearly active luminescent guest molecules. Moreover, a knowledge of the surface vibrational properties of the material as a function of the porosity can clarify the role of the pore curvature on the hydrogen-bond interaction between silanol structures.

Raman spectra of porous silica in the O–H stretching range (3000–3800 cm<sup>-1</sup>) display a broad band arising from the contribution of different hydrogen-bonding interacting hydroxyl species and a narrow feature at 3750 cm<sup>-1</sup> related to the O–H stretching in isolated silanols. As shown in Figure 1, the relative intensity of the isolated silanol band with respect to the broad band depends on pore size. It has been shown that decreasing the pore diameter increases the hydrogen-bonding interaction between neighboring structures and the hydrophilic nature of the samples (see ref 1 and references therein). This is well confirmed by Figure 1; the comparative analysis of samples with different pore size shows that the larger the pore diameter the larger the relative contribution of isolated silanols with respect to the interacting OH-species. To give an estimate of the water relative content in the samples, we analyzed the RS of liquid water (Figure 2) through Gaussian deconvolution; three components peaked at 3250, 3450, and 3610 cm<sup>-1</sup> have been attributed to the first overtone of the H<sub>2</sub>O bending, symmetric, and antisymmetric O–H stretching, respectively.<sup>12</sup> The liquid water simulated spectral profile, multiplied by a scaling factor, was used as a function to fit the RS of the three sets of samples in addition to Gaussian components; indeed, the vibrational properties of water nested into the pores are well reproduced by those of liquid water.<sup>14</sup> As shown in Figure 3 and Table 1, several vibrational contributions can be determined through the deconvolution of the RS spectra of the three sets of samples. Beside the adsorbed water composite band, contributions at about 3525, 3660, and 3750 cm<sup>-1</sup> have been singled out; their spectral positions do not depend on the mean pore diameter of the samples (see Table 1). These vibrational bands have been previously attributed to specific O–H stretching vibrations as follows: vibrations in the 3510–3540 cm<sup>-1</sup> range have been

associated to the SiO–H stretching of surface silanols hydrogen-bonded to molecular water.<sup>1,9–14</sup> O–H stretching in adsorbed water at the surface and mutually hydrogen-bonded SiOH stretching of surface hydroxyls have been attributed to the vibration peaked at 3660 cm<sup>-1</sup>. Furthermore, the 3520 and 3660 cm<sup>-1</sup> bands have been ascribed to stronger and weaker hydrogen-bonding in interacting OH-species.<sup>1</sup> As already stated, the 3750 cm<sup>-1</sup> is the fingerprint of the isolated silanol vibration.<sup>1,9–14</sup> A contribution in the 2800–3100 cm<sup>-1</sup> range is detected with peak position slightly dependent on the samples; the attribution of this feature is still open. Although the frequency of this stretch belongs to the C–H stretching range, preliminary X-ray photoelectron spectroscopy (XPS) measurements seem to exclude the presence of carbon in the analyzed samples. Moreover, a component peaked at 2965 cm<sup>-1</sup> has been distinguished through infrared spectroscopy in silica nanoparticles and associated to O–H stretching in adsorbed water dimers.<sup>18</sup>

In the O–H fundamental stretching range, sol–gel synthesized porous silica presents a variable relative concentration of H<sub>2</sub>O as a function of the porosity; as the pore diameter increases the relative content of adsorbed water decreases (Table 2). The relative contribution of the SiOH-related bands are found to be dependent on porosity through the analysis of integrated area percentage. By referring the interacting hydroxyl content to the isolated silanol one, their relative concentration is found to decrease as the sample pore diameter increases (Table 2). A pore curvature effect on the extent of hydrogen-bonding interaction between neighboring OH structures<sup>1</sup> can explain the observed effect; as the pore diameter decreases the hydrogen-bonding interaction between neighboring SiOH is enhanced and the relative concentration of interacting silanols increases with respect to the isolated ones. Furthermore, interacting silanols are preferential adsorption sites for water and polar molecules, and the relative content of adsorbed H<sub>2</sub>O increases by decreasing the pore diameter; smaller pores samples are more hydrophilic.

## 5. Conclusions

By studying the Raman spectra in the O–H stretching range of porous silica samples with different porosity, we detected a manifold vibrational activity and evidenced the specific contribution of surface silanols. A composite band in the 2900–3800 cm<sup>-1</sup> range and a narrow peak at 3750 cm<sup>-1</sup> are found. The spectral distribution of hydroxyl species giving rise to the detected bands is investigated as a function of the pore diameter of the samples through a standard best-fit deconvolution. Raman spectra are found to be the superimposition of several contributions: O–H vibrations from water molecules adsorbed at the surface, interacting silanols hydrogen-bonded to oxygen atoms of other silanols and/or adsorbed water molecules (3520 cm<sup>-1</sup>), mutually bonded SiOH species (3660 cm<sup>-1</sup>), and isolated SiO–H vibrations (3750 cm<sup>-1</sup>). The proposed analysis indicates a pore size and pore curvature dependence of the OH-species covering the porous silica surface. The relative concentration of adsorbed water and interacting silanols with respect to the isolated ones increases as the pore diameter decreases; smaller pore samples have an enhanced hydrophilic character.

**Acknowledgment.** This study has been supported by National Research Project of MIUR (Ministero dell'Istruzione, dell'Università e della Ricerca) and by INFN (Istituto Nazionale per la Fisica della Materia) of Italy.

## References and Notes

- (1) Brinker, J.; Sherer, G. W. *Sol–Gel Science—The physics and the chemistry of sol–gel processing*; Academic Press: San Diego, 1990.

- (2) Klein, L. *Sol-gel technology for thin films, fibers, preforms, electronics and specialty shapes*; Noyes Publications: Park Ridge, NY, 1988.
- (3) Hench, L. L.; West, J. K. *Chem. Rev.* **1990**, 90, 33.
- (4) McDonagh, C.; Bowe, P.; Mongey, K.; MacCraith, B. D. *J. Non-Cryst. Solids* **2002**, 306, 138.
- (5) Schulz-Ekloff, G.; Wöhrle, D.; van Duffel, B.; Schoonheydt, R. A.; *Microporous Mesoporous Mater.* **2002**, 51, 91.
- (6) Brinker, C. J.; Kirkpatrick, R. J.; Tallant, D. R.; Bunker, B. C.; Montez, B. *J. Non-Cryst. Solids* **1988**, 99, 418.
- (7) Allen, S. G.; Stephenson, P. C. L.; Strange, J. H. *J. Chem. Phys.* **1997**, 106, 7802.
- (8) Krol, M.; van Lierop, J. G. *J. Non-Cryst. Solids* **1984**, 63, 131.
- (9) Klein, L. C.; Gallo, T. A.; Garvey, G. J. *J. Non-Cryst. Solids* **1984**, 63, 23.
- (10) Gottardi, V.; Guglielmi, M.; Bertoluzza, A.; Fagnano, C.; Morelli, M. A. *J. Non-Cryst. Solids* **1984**, 63, 71.
- (11) Kinowski, C.; Bouazaoui, M.; Bechara, R.; Henc, L. L.; Nedelec, J. M.; Turrell, S. *J. Non-Cryst. Solids* **2001**, 291, 143.
- (12) Davis, K. M.; Tomozawa, M. *J. Non-Cryst. Solids*, **1996**, 201, 177, and references therein.
- (13) Morrow, B. A.; McFarlan, A. J. *J. Phys. Chem.* **1992**, 96, 1395.
- (14) Benesi, H. A.; Jones, A. C. *J. Phys. Chem.* **1959**, 63, 179.
- (15) Geltech Inc. (US), technical report.
- (16) Press, W. H.; Teukolsky, S. A.; Vetterling, W. T.; Flannery, B. P. *Numerical Recipes in C, The Art of Scientific Computing*, Second Edition; Cambridge University Press: Cambridge, 1992.
- (17) *Defects in SiO<sub>2</sub> and Related Dielectrics: Science and Technology*; Pacchioni, G., Skuja, L., Griscom, D. L., Eds.; Kluwer Academic Publishers: Dordrecht, 2000.
- (18) Anedda, A.; Carbonaro, C. M.; Clemente, F.; Corpino, R.; Grandi, S.; Mustarelli, P.; Magistris, A. *J. Non-Cryst. Solids* **2003**, 322, 68.
- (19) Glinka, Y. D.; Lin, S. H.; Chen, Y. T. *Phys. Rev. B* **2000**, 62, 4733.